Simulation of Composite Naval Plates Submitted to Gel Projectile Impacts

J.-C. PETITEAU[a], A. FAVRY[a], L. MARQUEZ[b], H. LE SOURNE[b, c], S. DURAND[a]

a. MÉCA, bureau d'études, Nantes, France – samuel.durand@calcul-meca.fr
b. Dept.of Mechanical Engineering, ICAM, Nantes, France
c. GeM Institute – UMR CNRS 6183, École Centrale de Nantes, France

Résumé :

Ce travail présente les résultats obtenus dans la caractérisation du comportement de plusieurs plaques composites navales soumises à des impacts de gélatine. Les plaques étudiées sont réalisées en stratifiés CFRP et GFRP. La simulation non linéaire explicite par éléments finis qui a été validée par des essais est basée sur l'interaction fluide-structure entre un impacteur avec des propriétés équivalentes à celles de l'eau qui est modélisée en utilisant une approche Arbitrary Lagrangian Eulerian (ALE) et une coque multicouche composite. Une loi matériau orthotrope avec un critère de rupture est ensuite utilisée pour évaluer les différents modes de rupture intra-laminaire qui peuvent se produire dans les plaques impactées, tels que la rupture des fibres, le flambage des fibres, la fissuration de la matrice et la rupture en compression de la matrice. Le critère de Chang-Chang-Chang est utilisé car il permet de séparer les différents modes de défaillance de la plaque composite.

Abstract:

This work presents the results obtained in characterizing the behavior of several naval composite plates submitted to gel impacts. The plates studied are made of CFRP and GFRP laminates. The nonlinear explicit finite element simulation that has been validated against impact tests is based on Fluid Structure Interaction between an impactor with water properties which is modeled using an Arbitrary Lagrangian Eulerian approach and a shell composite plate. An orthotropic material law with a failure criterion is then used for evaluating the different intra-laminar failure modes that may occur in the impacted plates such as fiber rupture, fiber kinking, matrix cracking and matrix compressive failure. The Chang-Chang Criterion is used as it enables to separate the different failure modes in the composite plate.

Mots clefs : Composite, Fluid Structure Interaction, Intra-laminar damage, Gel Impact

Nomenclature

γ_{xy}	Shear deformation
τ_{xy}	Shear stress
G_{xy}	Linear shear modulus, idem for $G_{//\perp}$
$G_{\|\perp s}$	Non-linear secant shear modulus
α	Non-linear shear coefficient
β	Parameter for Chang-Chang tensile fiber criterion
θ	Ply orientation
X_c	Maximum compressive stress in fiber direction
X_t	Maximum tensile stress in fiber direction
Y_c	Maximum compressive stress in transverse direction
Y_t	Maximum tensile stress in transverse direction
S_c	Maximum in-plane shear stress
f_E	Distance ratio between current state of stress vector and failure vector
f_{Ethr}	f_E value at the beginning of non-linear behavior
e_f	Tensile fiber failure criterion
e_c	Compressive fiber failure criterion
e_M	Tensile matrix failure criterion
e_d	Compressive matrix failure criterion

1 Introduction

The present work is part of the SUCCESS project which is a collaborative project funded by the French defense agency DGA, led by MECA with its partners ICAM and MULTIPLAST. Its objective was to develop new calculation and design methods for loading definition and coupled dynamic response of composite structures subjected to hydrodynamic impacts (slamming) and underwater explosions (UNDEX). Indeed, these two types of loading, are two of the most important design loads to be taken into account in naval engineering especially in the field of composite materials. Two main challenges are faced in designing this type of structure: to be able to model the behavior of naval structure submitted to these loads with computational costs compatible to industry needs and to characterize the material behavior under UNDEX or slamming. Indeed, performing experiments of these events is not only a costly but also a complicated and hazardous process. On the other hand, methods such as gas cannon testing are used in the aerospace industry, especially for bird strike tests. These soft body impacts use gel impactor that exhibit a behavior similar to the one of water and therefore can be of use in the field of ship design. Furthermore, this kind of tests is able to be used in combination with simulation to characterize the behavior of composite materials up to failure.

In the present work, impact tests and corresponding numerical simulations has been realized for three monolithic composite layups (two CFRP and one GFRP). Results given by the simulation are compared to the experimental ones and disparities are discussed in order to improve the accuracy of the model for further works.

2 Impact test to be modeled

The modeled experiment was conducted by G. Barlow and O. Dorival [1] as part of the same project and is briefly presented in Figure 1. It consists of simply supported composite plate impacted by a gel projectile thrown by a gas cannon. The composite plate is put on a steel plate with a hole which allows the deflection of the composite plate. The projectile speed varies between 60 m.s^{-1} and 110 m.s^{-1} and is measured thanks to a high-speed camera. The composite plate deformation is obtained using Digital Image Correlation (DIC).

Several composite layups are tested with two types of fiber/resin pair (T700 carbon fiber/epoxy and E glass fiber/vinylester) and different stacking sequences (oriented, cross-ply and quasi-isotropic laminates).

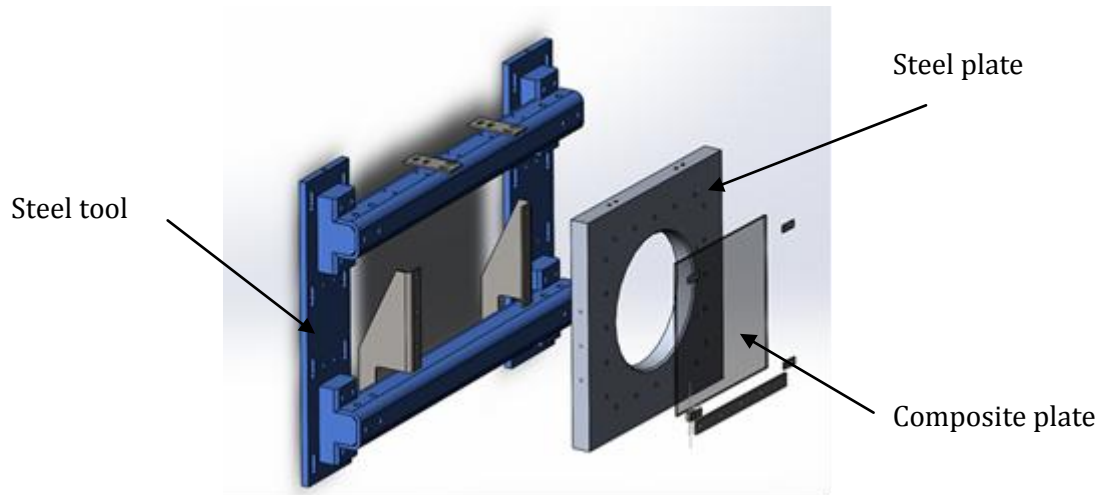The three tested samples are described in Table 1.

Steel tool

Steel plate

Composite plate

Figure 1 – Experimental setup

Sample #01 – Carbon/Epoxy			
Number of ply	Type of ply	θ (°)	Weight (g/m²)
1	Twill	+/-45	300
3	UD	0	300
1	Twill	+/-45	300
3	UD	0	300
4	UD	90	300
3	UD	0	300
1	Twill	+/-45	300
3	UD	0	300
1	Twill	+/-45	300

Sample #02 – Carbon/Epoxy			
Number of ply	Type of ply	θ (°)	Weight (g/m²)
1	UD	+45	300
1	UD	-45	300
1	UD	0	300
1	UD	90	300
1	UD	+45	300
1	UD	-45	300
1	UD	0	300
1	UD	90	300
1	UD	+45	300
1	UD	0	300
1	UD	90	300
1	UD	-45	300
1	UD	90	300
1	UD	0	300
1	UD	-45	300
1	UD	+45	300
1	UD	90	300
1	UD	0	300
1	UD	-45	300
1	UD	+45	300

Sample #03 – Glass/Vinylester			
Number of ply	Type of ply	θ (°)	Weight (g/m²)
1	Twill	0/90	300
14	Twill	0/90	600
1	Twill	0/90	300

Table 1 – Sample layup descriptions

3 Numerical model

3.1 LS-DYNA model

The different elements of the model are presented Figure 4. The steel plate is modeled as a rigid shell and is supposed to be clamped. Thus, the steel tool is not modeled. The composite plate is modeled as 3D-layered shell elements and a frictionless contact between those two plates is taken into account. Each layer of the composite layup is assumed to be a unidirectional ply. Thus, woven fabrics are modeled as a superposition of two unidirectional plies perpendicularly oriented. This hypothesis is needed in order to use phenomenological failure criteria.

The projectile is modeled using an Arbitrary Lagrangian Eulerian (ALE) mesh. The gel projectile behavior is modeled thanks to an elastic-plastic and hydrodynamic material law (*MAT_ELASTIC_PLASTIC_HYDRO) and a polynomial equation of state (EOS) which corresponds to water EOS. The behavior between the projectile and the impacted plate is ruled by a Fluid-Structure Interaction (FSI) model. Initial velocity is applied to the projectile.

3.2   Model accuracy

When a soft projectile impacts a rigid plate, its kinetic energy is transformed in both plate and projectile deformations. Moreover, when the projectile reaches the surface, there are two kind of pressure that are created inside the projectile: the stagnation pressure P_s and the Hugoniot pressure P_H. The last one is a very high compressive pressure due to the shock wave and depends mostly on the impactor density, the shockwave velocity and the impact velocity. The stagnation pressure depends only on the impact velocity and the projectile density. A typical impact force through time for a gelatin impact is shown in Figure 2 [2]. In order to check the model accuracy and the influence of the ALE mesh size, an impacted plate made of aluminum is assumed [3] and a comparison presented in Figure 3 with numerical [4] and experimental results [5] enables to validate the modelling of gel impactor and of the FSI approach used. Moreover, the results are compared to numerical results obtained by B.Wu in terms of stresses [6] as presented in Figure 5 and experimental results from Welsh experiment in terms of deflection [7] as presented in Figure 6. As the comparison show a good agreement between the results obtained by those authors and our results, the model used is validated.
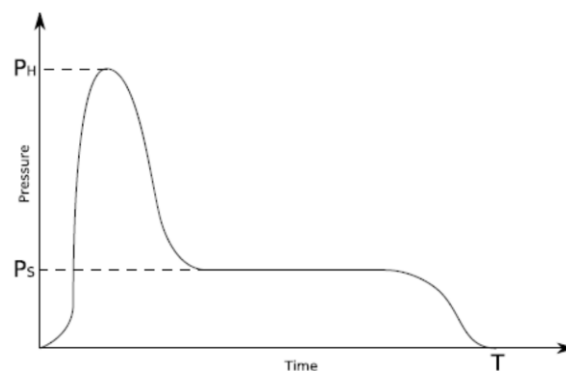

Figure 2 - Theoretical pressure output for a hydrodynamic impactor [2]
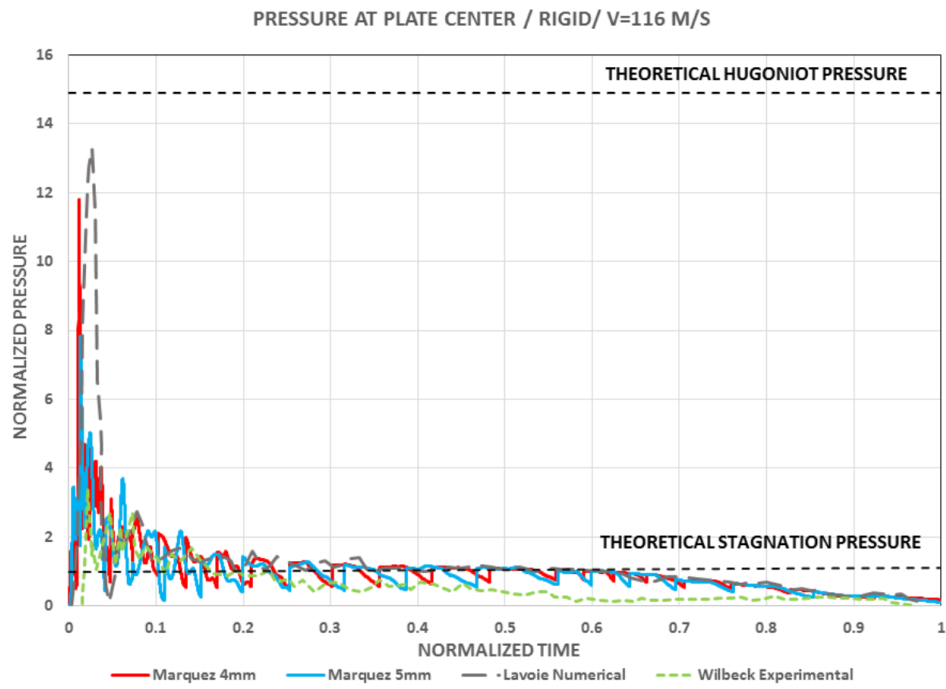
PRESSURE AT PLATE CENTER / RIGID/ V=116 M/S

Figure 3 - Comparison of pressure output for several numerical and experimental results

Figure 4 – Details of the LS-DYNA model

BO WU´S RESULTS   **PRESENT MODEL**

T= 0.42 MS

T= 1.08 MS
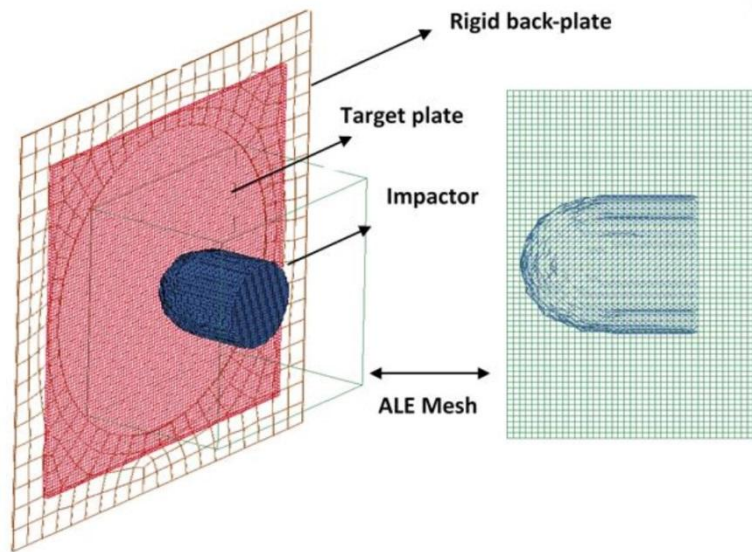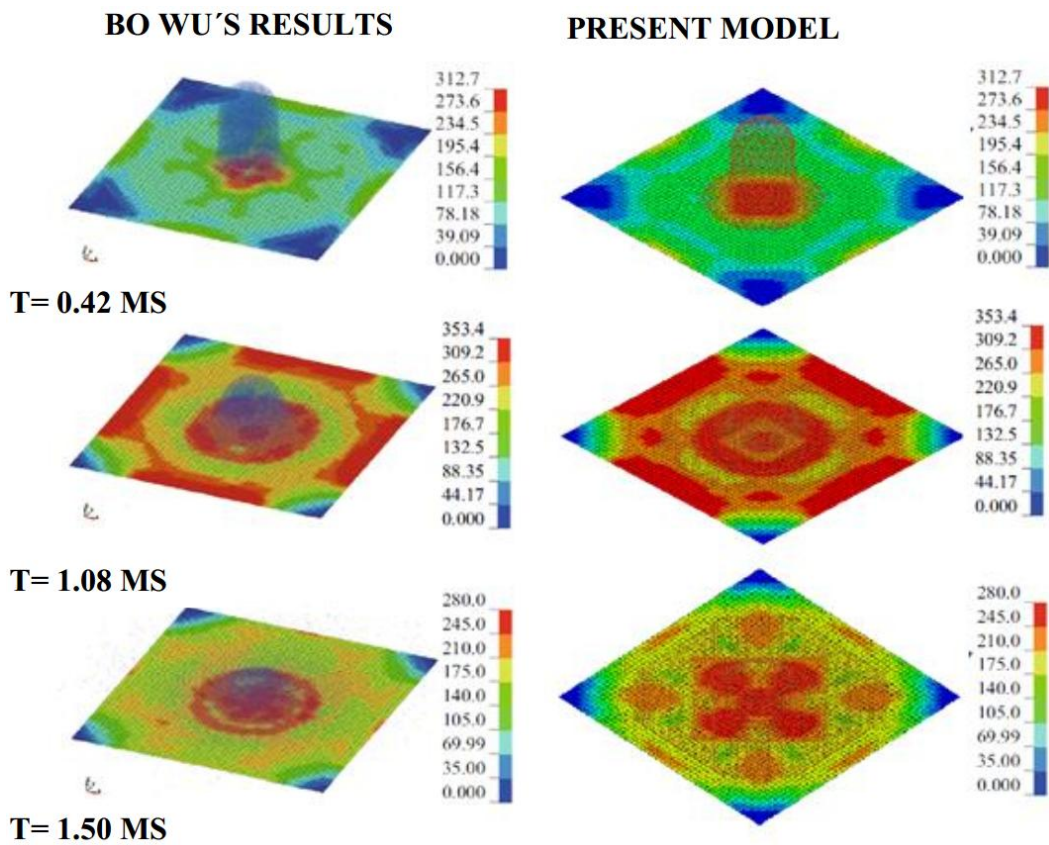
T= 1.50 MS

Figure 5 – Von Mises equivalent stress (MPa) comparison at several times between the B. Wu calculation [6] and the present model [3]
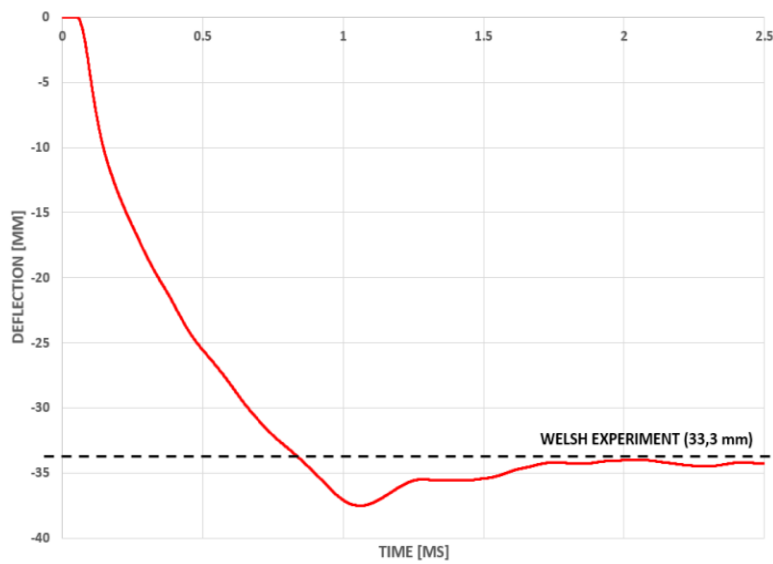
Figure 6 – Comparison between experimental maximum deflection [7] and numerical through time deflection [3] of the impacted plate

3.3   Material behavior of composites

3.3.1 Material law

Each sample is described with layers that contain the following information: material, thickness and orientation. Each layer is modeled by one through-thickness integration point in order to get reasonable calculation times. This allows to get strain, stress and damage variable maps at middle surface of each layer and at each time step.

As previously mentionned, the material card used in the model is MAT_54. This material law corresponds to an orthotropic material with composite failure criteria. The available failure criteria are Tsai-Wu or Chang-Chang criteria and the criteria used in this work is the Chang-Chang one [8].

3.3.2 Linear behavior

Material properties initially came from databases which gave a good estimation of linear properties. In order to get more accurate behaviors, hammer impact tests were conducted at Toulouse ICAM to determine the modal behavior of the plates. The results given by those experiments are compared to a finite element model and enable to adjust the modeled stiffness as shown in Table 2.

The model is made of a 3D-shell with homogenized properties thanks to the classical laminate theory. Properties are tuned in order to get the right modes at the right frequencies. Then, ply properties are deduced from modified global stiffness.

First, this method is applied to the sample #02 and #03 because each one is made of one type of ply: unidirectional plies for sample #02 and woven fabrics for sample #03. Then, since the first sample is made of both unidirectional plies and woven fabrics, changes are applied on each type of ply according to previous conclusions and the final stiffness is compared to the experimental results. Thus, the consistency of the results could be verified.
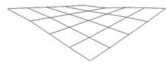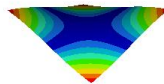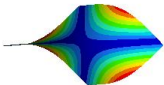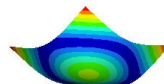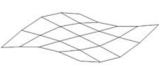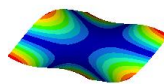
Mode number	Experimental results		Numerical results		Frequency ratio
	Mode shape	Mode frequency	Mode Shape	Mode frequency	
1		139 Hz		145 Hz	104%
2		170 Hz		172 Hz	101%
3		238 Hz		241 Hz	101%
4		339 Hz		349 Hz	103%

Table 2 – Comparison between experimental and model results with modified stiffness – sample #02

3.3.3 **Shear non-linear behavior**

The non-linear shear stress-strain relation used in the LS-DYNA MAT54 material law is the one proposed by Tsai and Hahn [9]:

$$\gamma_{xy} = \frac{\tau_{xy}}{G_{xy}} + \alpha \, \tau_{xy}^3 \tag{1}$$

This relation uses an α coefficient (in MPa^{-3}) which depends on different properties of the ply: type of fiber, resin fiber mass ratio, etc. Thus, values found in the literature cannot be used and shear tests are needed in order to get the right coefficient. In this project, no such experiments were conducted and the α coefficient estimation method is based on the works of Camanho [10] and Puck [11].

Camanho estimated the α coefficient of different laminates thanks to a least-square fit on test data from the World Wide Failure Exercise (WWFE). Figure 7 presents the shear behavior of those laminates according to Camanho's method (dotted line) compared to the WWFE data (points). The carbon fiber laminate shear behavior is well correlated compared to the behavior of the E glass fiber laminate which is very different from the prediction of the equation (1).

In the same figure, the behavior calculated from Puck's formulation (equation (2)) is plotted too (continuous line). This formulation seems accurate enough to give a good estimation of the shear non-linearity behavior.

$$G_{||\perp s} = G_{||\perp} - \left(\frac{\left[f_E^{(\tau_{21})} + C^{(\sigma_2)} \left(f_E - f_E^{(\tau_{21})} \right) \right] - f_{Ethr}^{(\tau_{21})}}{1 - f_{Ethr}^{\tau_{21}}} \right)^{n^{(\tau_{21})}} \left(G_{||\perp} - G_{||\perp s} \big|_{(f_E^{(\tau_{21})}=1)} \right) \tag{2}$$

Considering the maximum shear strain as the failure criterion, a comparison between the internal energies given by those two fitting methods gave the same results with a difference less than two percent. Thus, even if equation (1) with Camanho considerations does not lead to a perfect fitting of the shear behavior, the behavior at pure shear failure is well estimated with the right energy and at the right strain.

Since Puck's formulation gives a good estimation of the shear behavior, the method used in order to get the best shear non-linearity α coefficient is to fit the behavior given by Puck's formulation with Hahn and Tsai's equation (1) according to Camanho's method. According to the previous energy considerations, the failure criterion must be the maximum strain. However, the criterion used in LS-Dyna is a stress criterion. Hence, the shear strength taken into account is the stress corresponding to the maximum strain defined using Tsai and Hahn formulation.
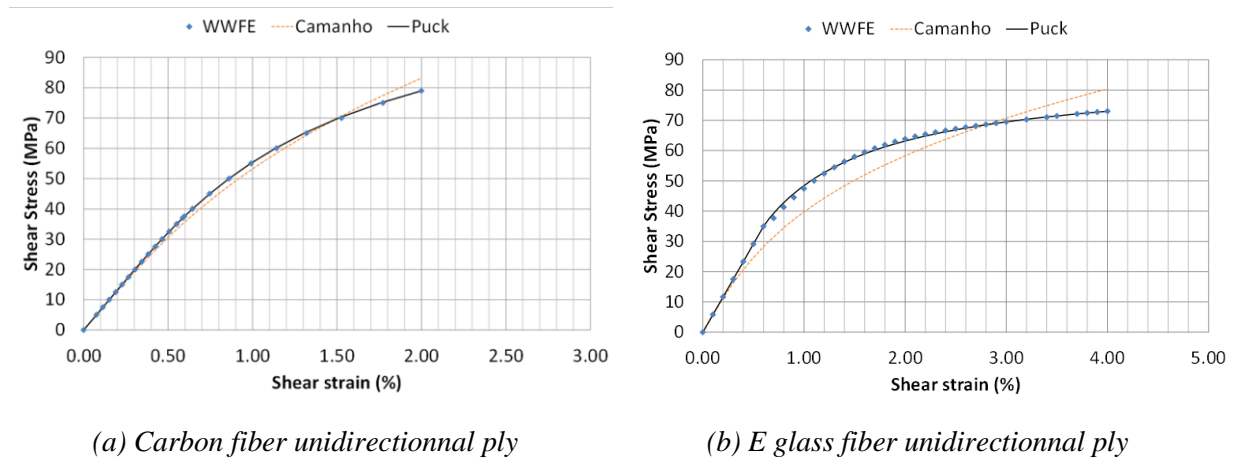
(a) Carbon fiber unidirectionnal ply   (b) E glass fiber unidirectionnal ply

Figure 7 – Comparison between Camanho and Puck methods and WWFE experimental data

3.3.4 Damage criteria and behavior

In MAT54, the damage criteria are called Chang-Chang criteria. In fact, the implemented criteria are slightly different and based on the work of Matzenmiller [12] as presented in Table 3.

In Chang-Chang criteria, S_c represents the maximum in-situ shear stress unlike in the MAT54 formulation where S_c represents the ply maximum shear stress. The in-situ effects are taken into account by the β coefficient which is defined as the square of the ratio of the ply shear resistance and the "in-situ" shear resistance (3). These considerations lead to the Hashin tensile fiber criterion [13] where the shear resistance is taken as the in-situ shear resistance. Assuming that the in-situ shear resistance is much higher than the ply shear resistance, β is negligible and the criterion is simplified and become a maximum stress criterion. These considerations are recommended by the LS-DYNA documentation [14] and are taken into account in the present model.

$$\beta = \left(\frac{S_c^{ply}}{S_c^{in-situ}} \right)^2 \tag{3}$$

Once a criterion is reached, the behavior of the material changes and there are several ways to model these changes depending on the failure mode which is triggered. In particular, a tensile failure mode leads to the failure of the ply because of the fragile behavior of the fibers. Numerically, this phenomenon leads to the deletion of the layer of the element. For tensile and compressive transverse and compressive fiber failure modes, the behavior after first damage is not fragile but is close to a plastic behavior: the stiffness decreases until the failure of the resin. In the present model, the chosen behavior of an element layer after one of those criteria is reached is a perfectly plastic behavior: the tangent modulus is zero.

Failure mode	Chang and Chang [8]	LS-DYNA MAT54 [14]
Tensile fiber	$e_f^2 = \left(\frac{\sigma_x}{X_t}\right)^2 + \dfrac{\frac{\sigma_{xy}^2}{2G_{xy}} + \frac{3}{4}\alpha\sigma_{xy}^4}{\frac{S_c^2}{2G_{xy}} + \frac{3}{4}\alpha S_c^4}$	$e_f^2 = \left(\frac{\sigma_x}{X_t}\right)^2 + \beta\left(\frac{\sigma_{xy}}{S_c}\right)^2$
Compressive fiber		$e_c^2 = \left(\frac{\sigma_x}{X_c}\right)^2$

Tensile matrix	$e_M^2 = \left(\dfrac{\sigma_y}{Y_t}\right)^2 + \dfrac{\dfrac{\sigma_{xy}^2}{2G_{xy}} + \dfrac{3}{4}\alpha\sigma_{xy}^4}{\dfrac{S_c^2}{2G_{xy}} + \dfrac{3}{4}\alpha S_c^4}$	$e_M^2 = \left(\dfrac{\sigma_y}{Y_t}\right)^2 + \left(\dfrac{\sigma_{xy}}{S_c}\right)^2$
Compressive matrix	$e_d^2 = \left(\dfrac{\sigma_y}{2S_c}\right)^2 + \left[\left(\dfrac{Y_c}{2S_c}\right)^2 - 1\right]\dfrac{\sigma_y}{Y_c}$ $\quad + \dfrac{\dfrac{\sigma_{xy}^2}{2G_{xy}} + \dfrac{3}{4}\alpha\sigma_{xy}^4}{\dfrac{S_c^2}{2G_{xy}} + \dfrac{3}{4}\alpha S_c^4}$	$e_d^2 = \left(\dfrac{\sigma_y}{2S_c}\right)^2 + \left[\left(\dfrac{Y_c}{2S_c}\right)^2 - 1\right]\dfrac{\sigma_y}{Y_c}$ $\quad + \left(\dfrac{\sigma_{xy}}{S_c}\right)^2$

Table 3 – Differences between Chang-Chang criteria and LS-DYNA MAT54 criteria

4 Results

4.1 Displacement comparison

Local and global displacements are compared through time. Figure 8 shows the comparison of the normal displacements at three different time steps with the same color scale for sample #02 impacted at 64m/s. For each time step, numerical plots are consistent with experimental results. In order to get a more precise comparison, Figure 9 shows the deflection at the center of the plate through time for the impact test and the numerical model. The impact occurs at 0 ms and the plate bends as the deflection increases until 1.4 ms when the center of the plate reaches the maximum deflection before decreasing with the same slope. After 3 ms the center of the plate does not move backward because the plate is simply supported.

The time response and maximum deflection are matching. The accuracy of the model seems fine as the initial slopes are parallels the same during the first 0.7 ms. From this time, there is a decrease of the slope that does not occur in the model. Once the maximum deflection is reached, the slope corresponding to the decrease of the deflection seems higher in the model that experimentally. These remarks lead to assume that damage occurs around 0.7 ms and increases the response time of the plate.
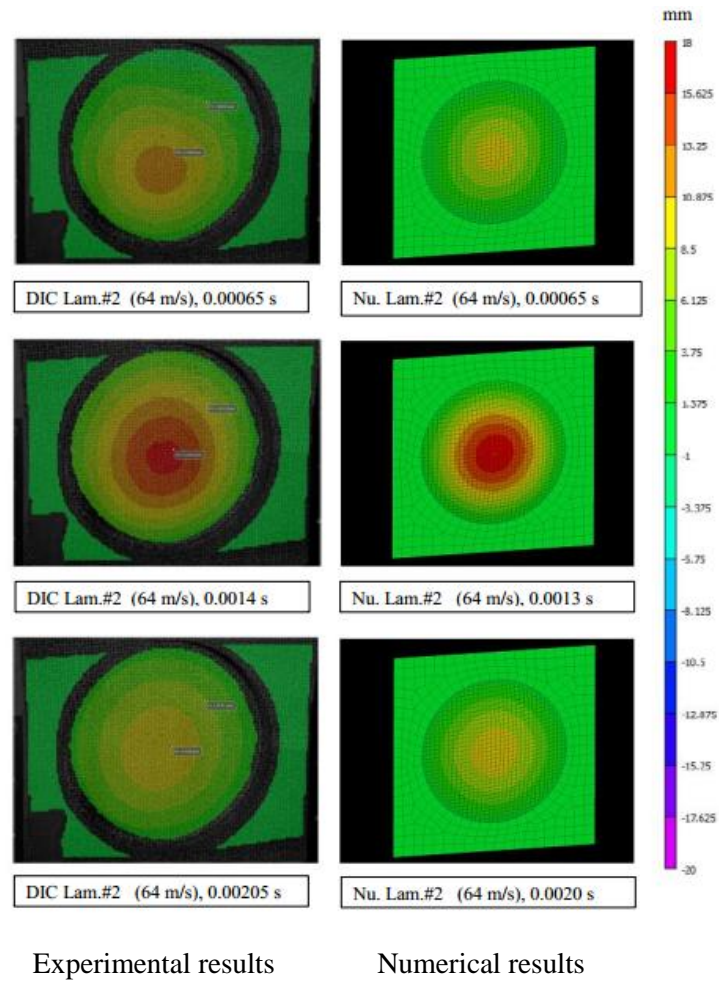
Experimental results   Numerical results

Figure 8 – Comparison bewtween experimental and numerical displacement of the composite plate at several timesteps – sample #02
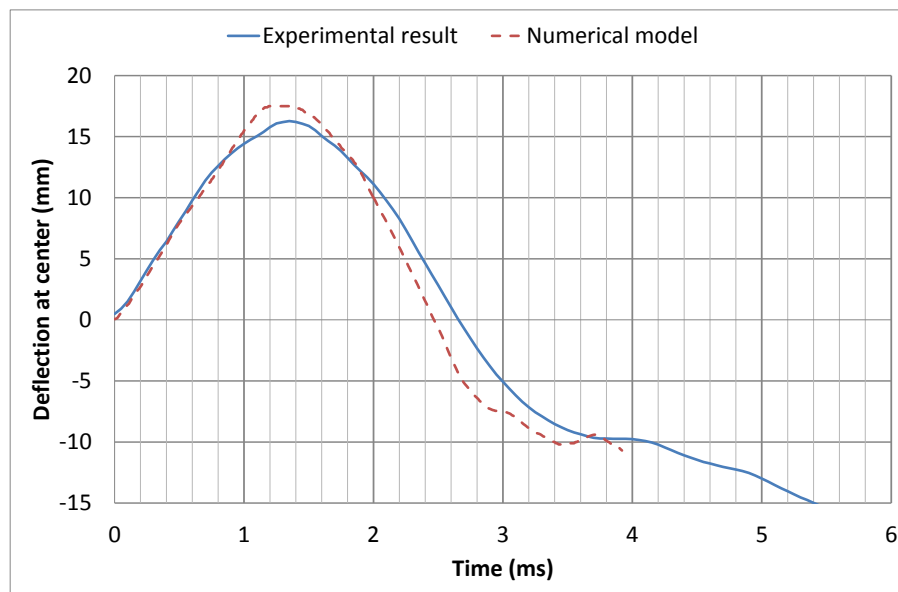

Figure 9 – Comparison between experimental and numerical deflection at the center of the plate – sample #02 with v=64 m/s

4.2   Damage

During this analysis, only tensile transverse failure modes occur. For the sample #02, the concerned plies are the five first bottom plies. The failure is due to the flexural behavior of the plate: bottom plies are highly stressed in tensile direction. The top plies are stressed too but failure does not occur since the ply compressive strengths are much higher than the tensile ones.

According to the numerical results (Figure 10), the failure begins at 0.5 ms for the bottom ply and spreads until 0.6ms (first two plies only). It starts spreading again at 0.99 ms and the third ply starts to be damaged at 1.05 ms before the fourth ply which starts damaging at 1.08 ms. Every damage spreading stops around 1.39 ms, right after the deflection reaches its maximum value (Figure 9). Moreover, it is interesting to note that damage starts around the same time the experimental slope decreases and confirms the previous hypothesis. A simulation without damage behavior was computed in the same time and highlighted that damage mechanisms, as modeled in these analyses, does not have significant influence on deflection.
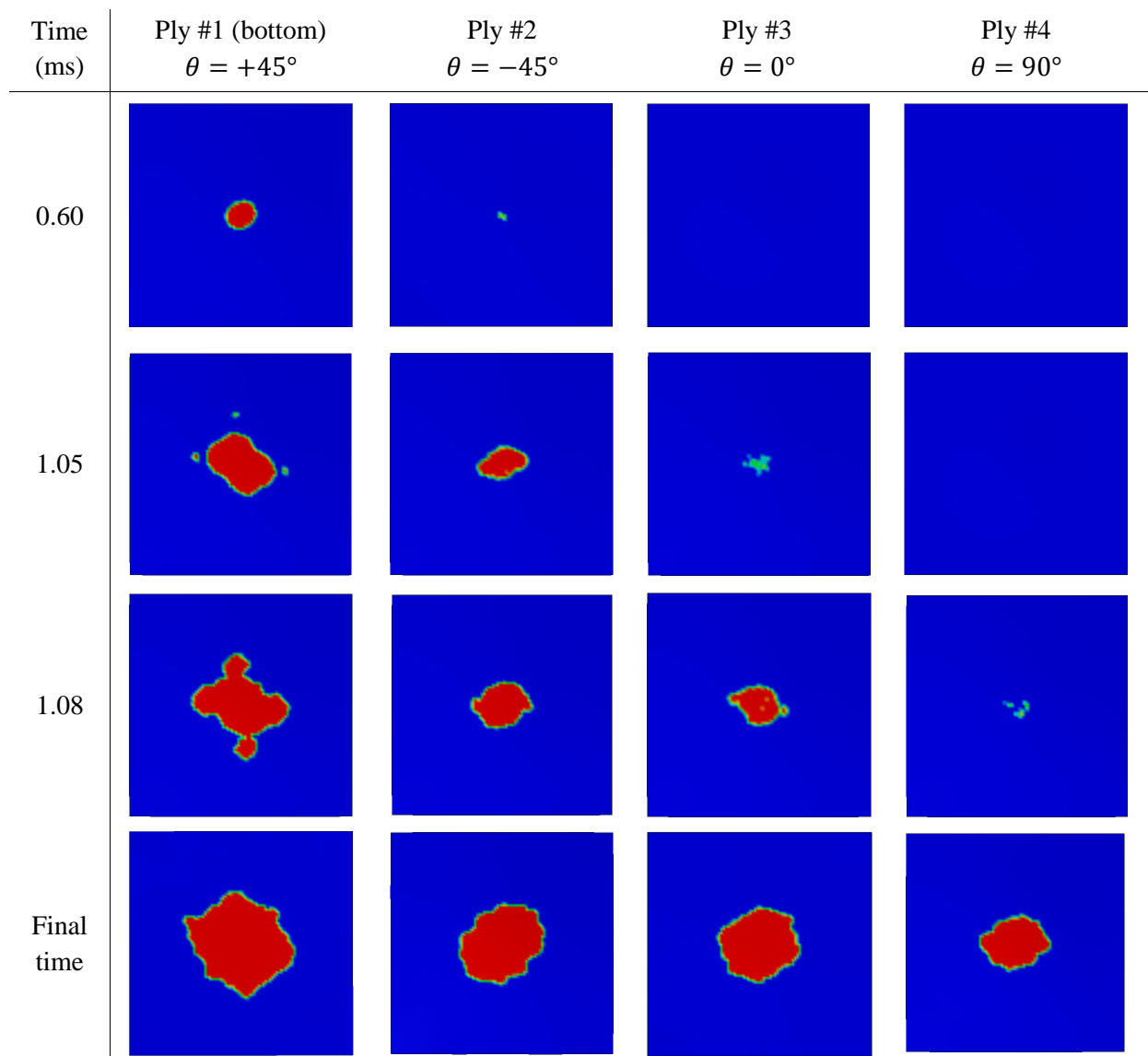
Time (ms)	Ply #1 (bottom) $\theta = +45°$	Ply #2 $\theta = -45°$	Ply #3 $\theta = 0°$	Ply #4 $\theta = 90°$
0.60				
1.05				
1.08				
Final time				

Figure 10 - Tensile transverse criteria (red=exceeded) for different plies at several time steps – sample #02 with v=64 m/s

5 Conclusion and further works

The model presented in this article gave consistent results compared to the experimental ones in terms of displacement. This model enables the composite plate behavior submitted to gel impact to be better understood.

Some issues due to the experimental setup can interfere with the result interpretation: uncentered impacts, condition of the projectile before impact, disparity of the samples. Part of the further works will be to decide which tests can be used as standards. Moreover, the presented model does not take into account dynamic effects on material stiffness which are known to be significant for fiberglass laminates especially. Furthermore, the present work only focused on monolithic composite layups but impact tests with sandwich panels made of GFRP skins and PET foam were conducted at Toulouse ICAM. Once the behavior of the monolithic samples is fitted, next studies will focus on those layups too.

Further works previously mentioned will permit the model to be more reliable and to fit more types of laminate.

6   Acknowledgement

References

[1] G. Barlow, O. Dorival, Comparaison des endommagements de composites sous impacts de gélatine et sous explosion sous-marine, 2019

[2] A. Blair, Aeroengine Fan Blade Design Accounting for Bird Strike, Ind. Eng., March (2008)

[3] L. Marquez, Implementation of the Arbitrary Lagrangian Eulerian Method in Soft Body Projectile Impacts against Composite Plates, Thèse de master, 2019

[4] M. Lavoie, A. Gakwaya, M. Nejad Ensan, D. G. Zimcik, Validation of Available Approaches for Numerical Bird Strike Modeling Tools, In. Rev. Mech. Eng., vol. 1, n°4 (2007) 380-389

[5] J. Wilbeck, Impact Behavior of low strength projectlies, vol. 5, n°c (1978) 107-109

[6] B. Wu, Z. Chen, X. Zhang, Y. Liu, Y. Lian, Coupled Shell-Material Point Method for Bird Strike Simulation, Acta Mech. Solida Sin., vol. 31, no.1 (2018) 1-18

[7] C. J. Welsh, Aircraft transparency Testing – Artificial Birds technical reports Arnold air force station, Tennessee air force systems command, 1986

[8] F.-K.Chang, K.-Y. Chang, A Progressive Damage Model for Laminated Composites Containing Stress Concentration, 1986

[9] H. T. Hahn, S. W. Tsai, Nonlinear Elastic Behavior of Unidirectional Composite Laminate, Journal of Composite Materials, vol.7 (1973) 102-118

[10] P. Camanho, Prediction of in situ strengths and matric cracking in composites under transverse tension and in-plane shear, Composites: Part A 37 (2006) 165-176

[11] A. Puck, M. Mannigel, Physically based non-linear stress-strain relations for the inter-fibre fracture analysis of FRP laminated, Composites Science and Technology 67 (2007) 1955-1964

[12] A. Matzenmiller, K. Schweizerhof, Crashworthiness simulations of composite structures – a first step with explicit time integration, 1991

[13] Z. Hashin, Failure Criteria for Unidirectional Fiber Composites, Journal of Applied Mechnanics, Journal of Applied Mechanics, vol. 47 (1980) 329-334

[14] Livermore Software Technology Corporation, LS-DYNA Keyword User's Manual, 2017